Optics and Laser Technology 129 (2020) 106281

Contents lists available at ScienceDirect

Optics and Laser Technology

journal homepage: www.elsevier.com/locate/optlastec

Highly efficient LD-pumped 607 nm high-power CW Pr^{3+}: YLF lasers

Xiuji Lin, Yao Zhu, Shuaihao Ji, Wensong Li, Huiying Xu, Zhiping Cai*

Department of Electronic Engineering, Xiamen University, Xiamen 361005, China

HIGHLIGHTS

- 4.88 W highest power of 607 nm CW laser based on Pr^{3+}:YLF crystals was achieved.
- 49.1% highest slope efficiency of 607 nm CW laser based on Pr^{3+}:YLF crystals pumped by blue laser diodes was achieved.
- Best beam quality of 607 nm Pr^{3+}:YLF CW laser was achieved under 3.80 W high power level.

ARTICLE INFO

Keywords:
Pr^{3+}:YLF crystal
Orange laser
High power
High efficiency

ABSTRACT

We demonstrated a 607 nm high-power continuous-wave (CW) orange laser based on a 12-mm-long a-cut Pr^{3+}:YLF crystal with high slope efficiency and a low doping level. A maximum output power of 4.88 W with a slope efficiency of ~49% was achieved at an absorbed pump power of 12.15 W, and no output saturation power was observed. To improve the laser beam quality, we designed a concave-plane cavity and achieved an output power of 3.80 W with M^2 factors of ~1.7 and ~2.2 in the horizontal and vertical directions, respectively, by means of a novel output coupler with tunable transmission. In addition, theoretical analyses were conducted to explain our designs, and the corresponding simulated results were presented.

1. Introduction

Approximately 600 nm high-power lasers are in great demand in many fields, such as biomedical applications [1,2], laser displays [3], metal processing [4], optical communication [5], and deep UV generation [6]. The primary method of generating approximately 600 nm high-power lasers is currently nonlinear frequency conversion, which is mainly based on nonlinear materials, including KTP, LBO, BBO, and LiNbO3 by sum-frequency generation [7–10], and other materials by the Raman effect [11,12]. However, such systems based on nonlinear frequency conversion are inefficient, complex, and expensive. Optically pumped semiconductor laser (OPSL) technology is another promising method to generate yellow-orange lasers, but it is expensive, complicated, and challenging to generate over 600 nm lasers [13]. Lasers based on organic dyes are also proven technologies in this wavelength region, but the short lifetime of dyes is an inherent disadvantage. Therefore, laser diode (LD)-pumped yellow-orange lasers based on Pr^{3+}-doped materials are recently developed solutions due to their advantages of high efficiency, simplicity, and low cost. Many Pr^{3+}-doped materials with large stimulated emission cross sections in the visible region, such as Pr^{3+}:ZBLAN [14,15], Pr^{3+}:YLF [16–18], and Pr^{3+}:YAP [19–21], have proven to have high potential. Among these materials, Pr^{3+}:YLF crystals have attracted much interest over the past decade for the generation of approximately 600 nm lasers since the low phonon energy contributes to excellent visible laser performance. However, high-efficiency 604 nm and 607 nm orange lasers are difficult to obtain due to reabsorption losses ($^3H_4 \rightarrow {}^1D_2$), especially when pumped by an LD array due to the low pump-beam quality. To date, the highest output power at 607 nm based on Pr^{3+}:YLF crystals has been reported as 3.7 W (Tanaka et al. [22]) but with inferior beam quality and a relatively low slope efficiency. In 2013, to achieve high efficiency under LD pumping, Xu et al. [23] proposed a design by pump beam reshaping and achieved a slope efficiency of 42% but with low output power.

In this work, we demonstrated CW high-power and high-efficiency 607 nm orange Pr^{3+}:YLF lasers under direct diode pumping at ~ 444 nm. Two types of experiments were implemented separately. In experiment 1, we designed a 51-mm-long laser cavity with two 50 mm radius-of-curvature plano-concave mirrors and output couplers (OCs) with transmissions of 4.4%, 5.4%, and 7.3% at 607 nm. A maximum output power of 4.88 W with a slope efficiency of ~49% was achieved based on an OC with 4.4% transmission. To the best of our knowledge, under blue LD pumping, the power and slope efficiency have maximum values. In experiment 2, we produced a 3.8 W high-

* Corresponding author.
E-mail address: zpcai@xmu.edu.cn (Z. Cai).

https://doi.org/10.1016/j.optlastec.2020.106281
Received 4 November 2019; Received in revised form 7 April 2020; Accepted 9 April 2020
Available online 25 April 2020

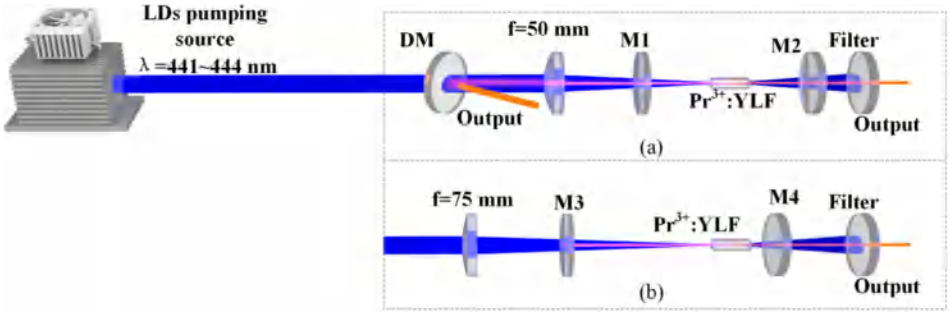

Fig. 1. Schemes of the LD pumped 607 nm CW Pr^{3+}:YLF orange laser. (a) Experiment 1: 4.88 W high power and ~49% high-efficiency orange laser. (b) Experiment 2: 3.80 W high power orange laser with improved beam quality.

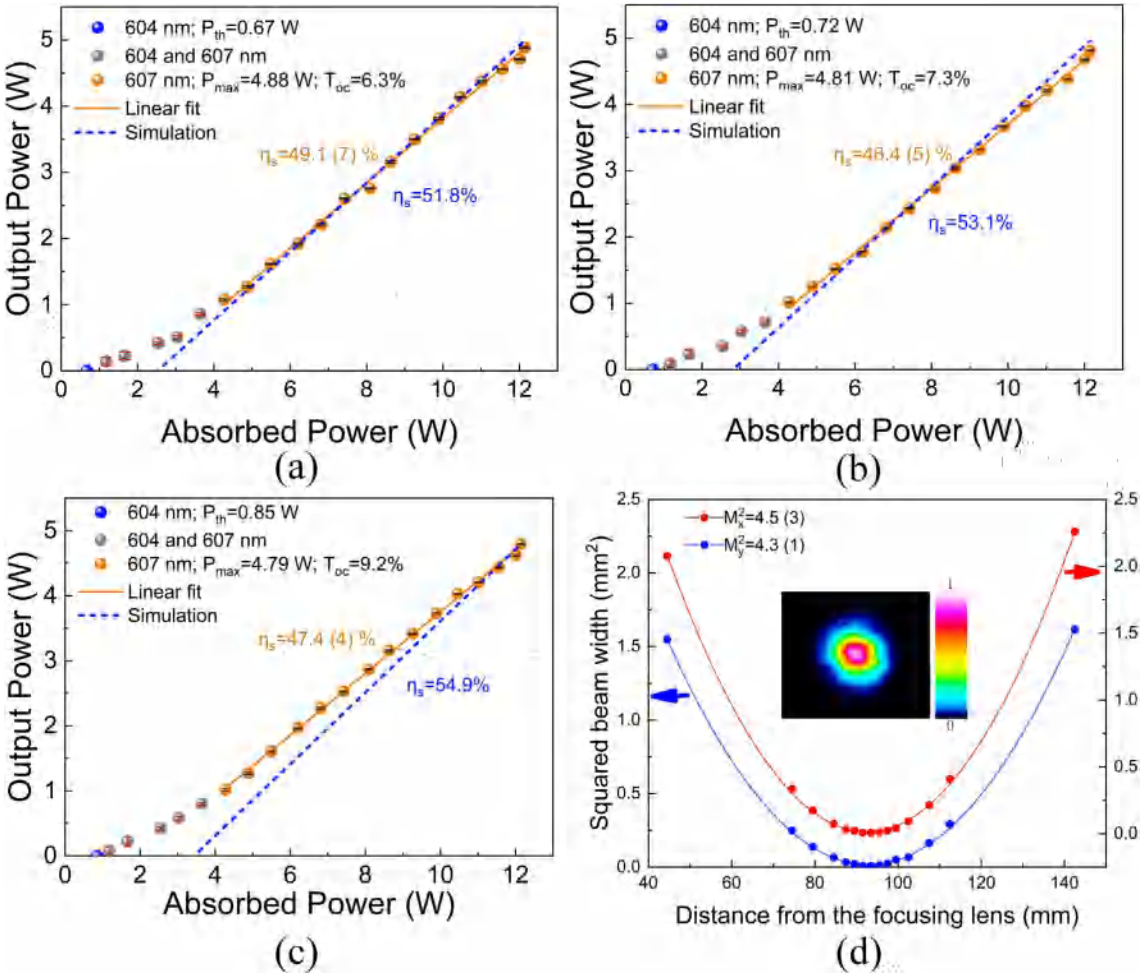

Fig. 2. Results of Experiment 1: Output power characteristics with three different OCs (M2). The orange lines represent linear fits; the blue and red lines represent polynomial fits; the dashed lines represent the simulation results. P_{th} indicates the power of the laser threshold; P_{max} indicates the maximum output power; T_{oc} indicates the transmission of the output coupler. The resolution of the power meter is 10 mW. (a) T_{oc} = 6.3%. (b) T_{oc} = 7.3%. (c) T_{oc} = 9.2%. (d) M^2 factors measured at the highest power of 4.88 W (the spot size stability is within 5%). The blue arrow indicates the y-scale of the blue line, and dots are on the left; the red arrow has a similar meaning.

power orange laser with an improved beam quality, which was achieved by a 72-mm-long concave-plane cavity with a 100 mm radius-of-curvature plano-concave input mirror (IM) and a plane OC with tunable transmission. Moreover, theoretical analyses and simulations were applied to explain the experimental results.

2. Experimental setups

As shown in Fig. 1(a), a commercially available InGaN LD array emitting at a peak wavelength of ~ 444 nm with a 24 W rated maximum power was used as the pumping source. The M^2 factors of the beam were calculated to be 15.53 and 46.91 in the horizontal (x) and vertical (y) directions, respectively, on the basis of the parameters provided by the manufacturer. An aspherical plano-convex lens with a 50 mm focal length was used to focus the pump beam into the crystal. A simple end-pumped resonator with two plano-concave spherical mirrors was set up to achieve a high-power high-efficiency 607 nm laser. An available mirror with a transmission of 1.9% at 607 nm and high transmission at red wavelengths was used as an input coupler (M1) for red oscillation suppression. We applied a set of OCs (M2) with three

different transmissions at 607 nm and high transmission at green wavelengths for the elimination of green oscillation to optimize the performance. Both M1 and M2 had 50 mm radii of curvature and were placed symmetrically around the 12-mm-long a-cut Pr^{3+}:YLF crystal with 3 × 3 mm^2 polished facets. The physical cavity length was carefully optimized to 51 mm to achieve the best performance. To reduce unwanted reabsorption losses, we utilized a crystal with low doping levels here. The doping concentration of Pr^{3+} ions was expected to be 0.2 ± 0.1 at. % (atomic percentage) and was measured to be approximately 0.15 at. % by comparing it to a 0.5 at. % Pr^{3+}-doped YLF sample. Because the full width at half maximum of the pump LD was 2.2 nm, the peak absorption efficiency of the crystal was relatively low (~51%). The crystal was wrapped with indium foil and then mounted inside a water-cooled copper block. The temperature of the water was set to 3℃ to reduce the detrimental thermal effects. A dichroic mirror (DM) with high transmission at blue wavelengths and high reflection at orange wavelengths was positioned between the focusing lens and the pump source to separate orange lasers from the pump light since the relatively high transmissivity of M1 at 607 nm could lead to a non-negligible output on the input side.

To improve the beam quality, as Fig. 1(b) shows, we proposed a concave-plane cavity consisting of a plano-concave mirror (M3) with a 100 mm radius-of-curvature as the input coupler and a plane mirror (M4) as the OC to suppress high order transverse modes. The home-made M4 with a gradationally thick dielectric coating, which could result in different transmissions of the target laser wavelength, was applied to optimize the laser performance. The laser transmission at 607 nm was measured from 8.9% to ~ 80%. The optimized cavity length was 72 mm. Here, the focus lens was replaced by one with a 75 mm focal length to reduce thermal effects and inhibit degeneration of the laser beam.

3. Results and discussion

In Experiment 1, we obtained the highest output power of 4.88 W with the highest slope efficiency of ~49% (the standard deviation is 0.7%) by an OC with a 4.4% transmission at 607 nm (see Fig. 2(a)). Two different OCs with 5.4% and 7.3% transmissions were also used, resulting in output powers of 4.81 W and 4.79 W, respectively, and slope efficiencies of ~48% and ~47%, respectively (the standard deviations were 0.5% and 0.4%, respectively), as shown in Fig. 2(b) and (c), respectively. It should be noted that T_{oc} in Fig. 2 indicates the total transmission of the IM and OC. At the beginning of the laser operation, the lasing wavelengths were all 604 nm. With increasing absorbed pump power, dual-wavelength operation at 604 nm and 607 nm was observed. As the absorbed power increased to 4.3 W, a single lasing wavelength of 607 nm was observed. Finally, the maximum output powers were obtained at the highest absorbed power of 12.15 W (the output power of the LD array was measured to be 26.50 W, and an approximately 10% loss of pump power was introduced mainly by three mirrors between the pump source and the crystal). Due to a slightly higher actual emission cross section (after excluding the influence of reabsorption) at 604 nm (19.6 × 10^{-20} cm^2) than at 607 nm (15.7 × 10^{-20} cm^2) measured at room temperature (Fig. 3), we first obtained 604 nm lasers of under the condition of low reabsorption losses (low doping concentration) and almost the same output coupling losses. YLF crystals exhibit different thermal lensing effects in the σ and π directions due to the different thermal expansion coefficients (8 × 10^{-6} and 13 × 10^{-6} K^{-1} at π and σ [24]) and negative coefficients dn/dT (-4.3 × 10^{-6} K^{-1} for π and −2.0 × 10^{-6} K^{-1} for σ [24]). Therefore, for the 604 nm emission of π, the negative thermal lensing effects were much stronger than the 607 nm emission of σ, which is attributed to the higher refraction change corresponding to the temperature and lower compensation of the positive thermal lensing effects from surface expansion. When the pump power increases, the thermally induced losses at 604 nm increase faster than the losses at 607 nm based on previous

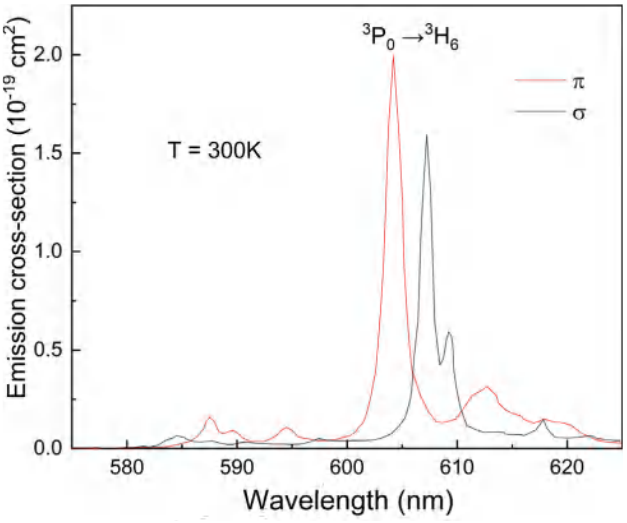

Fig. 3. Emission cross section of Pr:YLF in the orange region. π indicates that the polarization direction of emission is parallel to the optical axis. σ indicates that the polarization direction of emission is perpendicular to the optical axis.

analyses. In the process of optimization, we also found that when the temperature of the water cooling system was set to 20 ℃, the 604 nm single emission disappeared. Therefore, we considered that the thermally induced losses were the main reason that the laser wavelengths varied from single emission at 604 nm to 604/607 nm dual-wavelength emission and then to single emission at 607 nm. This explanation was also supported by the apparent shifting trends observed in Experiment 2 below (see Fig. 4(a)) since the longer focal length of the focus lens would lead to weaker thermal lensing effects.

The M^2 factors were measured to be ~4.5 and ~ 4.3 (the standard deviations are 0.3 and 0.1, respectively) in the *x* and y directions, respectively, by a focus lens and a CCD in the visible range at the highest power of 4.88 W (see Fig. 2(d)). Since there was a slight variation in the horizontal angle between the direction of propagation of the surface of the CCD when moving the CCD, the standard deviation in the horizontal direction was slightly larger than that in the vertical direction. The M^2 factors indicate poor beam quality, although the energy distribution of the beam showed a nearly Gaussian pattern. To perform the simulation, we calculated the spot radius (for an imperfect round beam, we could use the half-width instead of the radius to characterize half the width of the beam in a specific direction) in the active medium through [23]

$$w\ z = w0\sqrt{1 + \left(\frac{\lambda M^2 z}{\pi w_0^2}\right)^2}$$

where M^2 is the beam propagation factor, w_z is the measured beam radius, and z is the distance between the measuring location and the waist of the beam. The half-widths of the actual laser beam in the crystal at the highest power of 4.88 W were calculated to be 272 and 313 μm in the x and y directions, respectively.

The results were also simulated by applying the elliptic Gaussian pumping theory from Laporta [25] because of the asymmetry in the x and y directions of the pumping beam. The normalized pump distribution can be given by

$$g_e(x, y, z) = K_e \exp(-2\frac{x^2 + \beta^2 y^2}{\bar{w}_{pe}^2} - az)$$

where $\bar{w}_{pe} = \min\{\bar{w}_{px}, \bar{w}_{py}\}$, $K_e = 2\alpha\beta/[\pi\bar{w}_{pe}^2(1 - \exp(-al))]$, $\alpha = (w_l/\bar{w}_{pe})^2$, β is defined as the ratio of the minor to major beam size ($0 < \beta \leqslant 1$), a is the absorption coefficient, and w_l is the half-width of the waist of the output laser beam in media. $\bar{w}_p$ is the root mean square of the pump beam in active media, which can be defined as [26]

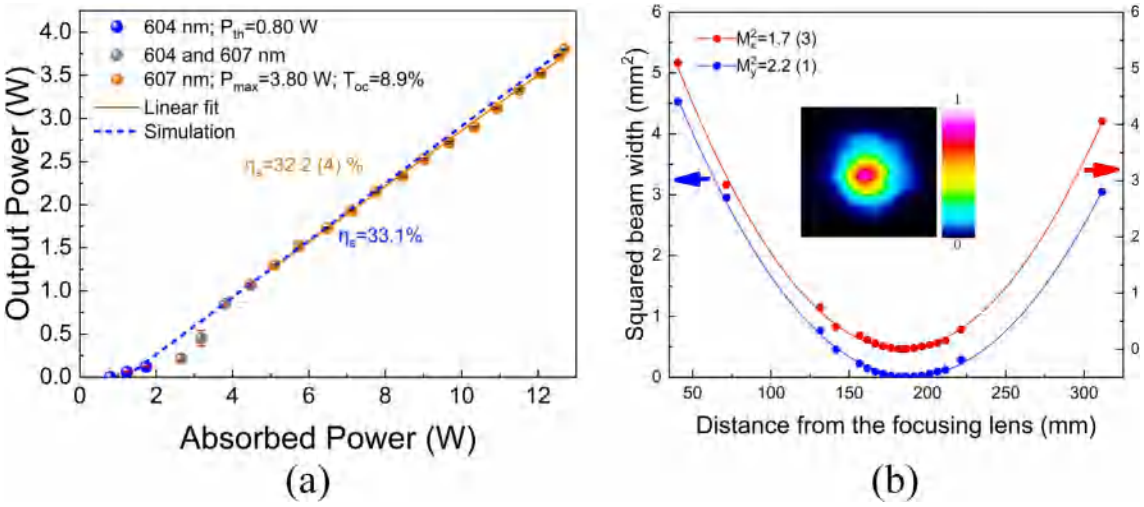

Fig. 4. Results of Experiment 2: Output power characteristics with the plane OC (M4). The explanations of the notations are the same as those in Fig. 2. (a) T_{oc} = 8.9%. The dashed line shows the simulation results. The resolution of the power meter is 10 mW. (b) M^2 factor measurement at the highest power of 3.80 W (the spot size stability is within 5%). The explanations of the arrows are the same as those in Fig. 2(d).

$$\bar{w}_p(z) = \sqrt{\frac{\int_0^l w_p^2(z)\exp(-az)dz}{\int_0^l \exp(-az)dz}}$$

where l is the length of the crystal along the z-axis (the optical axis) of the laser system. The power of the output laser can be given by [25]

$$P_{out} = (\frac{T}{2\gamma})\eta_p P_{tho} f_1(\alpha,\beta)(P_{abs}/P_{tho} - f_0(\alpha,\beta))$$

where T is the total transmissivity of the output coupler, γ is the total single-pass loss of the laser,

$$f_0(\alpha,\beta) = [(\alpha\beta^2+1)(\alpha+1)]^{1/2}/\beta f_1(\alpha,\beta)$$
$$= \alpha\beta[(\alpha\beta^2+2)(\alpha+2)]^{1/2}/[(\alpha+1)(\alpha\beta^2+1)]$$

indicate the overlap efficiency and $\eta_p = \eta_t\eta_a(\nu_l/\nu_p)$ is the pump efficiency, where η_t is the optical transfer efficiency, η_a is the absorption efficiency, and ν_l and ν_p are the frequencies of the laser and pump photons, respectively. We could take η_p to be the Stokes' efficiency which is defined as ν_l/ν_p since the optical transfer efficiency could be assumed to be 1, and we used the absorbed power in the calculations. $P_{tho} = \pi\gamma I_{sat}\bar{w}_{pe}^2/2\eta_p$ where I_{sat} is the saturation intensity. From previous analyses, we can see that the high overlap efficiency and low intracavity losses are vital parameters to achieve high power and high slope efficiency. Through calculations, we obtained a maximum f_1 of 90.6%, and the internal round-trip losses were estimated as less than 1.16% when T_{oc} = 6.3%. The parameters in the simulation are listed in Table 1. The reflectivity of the YLF crystal at ~ 600 nm (R_c) is given to correct the transmission considering the Fabry-Perot condition [27]. The simulated results are shown in Fig. 2, and we can see that both the slope efficiencies and output powers are slightly higher than the experimental values since the overlap efficiency should actually be lower than the theoretical value due to the deviation of the pump beam from the elliptical Gaussian distribution. Then, we can see that the variation in the trend of slope efficiencies is not the same between the experimental and simulated results. The reason may be that the lower intracavity power at 607 nm would lead to higher reabsorption losses. Therefore, the higher transmission may not result in a higher slope efficiency as expected.

In Experiment 2, as shown in Fig. 4, we improved the quality of the output laser beam by a longer hemispherical cavity with a plano-concave mirror with a 100 mm radius of curvature. We achieved an output power of 3.80 W with a slope efficiency of ~ 32% at an absorbed power of 12.65 W, and the M^2 factors were measured to be ~ 1.7 and ~ 2.2 (the standard deviations were 0.3 and 0.1, respectively) in the × and y directions, respectively (a significant improvement compared with [22]). The better beam quality could be considered mainly to the reduction of transverse modes (the beam half-widths were measured as 95 and 128 μm in the x and y directions, slightly larger than the TEM_{00} mode). Lower output power was obtained mainly due to the lower maximum overlap efficiency (calculated as 59.1%) and higher intracavity losses (internal round-trip losses were estimated less than 1.68%). The parameters in the simulation are listed in Table 2. Correspondingly, simulated results are also shown in Fig. 4(a), which are based on the same theoretical analyses as Experiment 1.

Table 1
Parameters used in the simulation in Fig. 2(a), (b) and (c). R_c is the reflectivity of the YLF crystal at ~600 nm.

T_{oc} (%)	γ	η_p	P_{tho} (W)	f_1	f_0	R_c (%)
6.3	0.028	0.732	0.207	0.906	12.204	3.7
7.3	0.031	0.732	0.230	0.906	12.204	3.7
9.2	0.038	0.732	0.281	0.906	12.204	3.7

4. Conclusion

We demonstrated a promising LD-pumped high-power (4.88 W) and high-slope-efficiency (~49%) design of laser emitting at 607 nm based on a Pr^{3+}:YLF crystal. To the best of our knowledge, the power and slope efficiency of the laser at 607 nm are the highest yet achieved under LD pumping. Beam quality (M^2 factors were measured as ~1.7 and ~2.2 in the x and y directions) was significantly improved with high output power (3.80 W) at the same time. Finally, we also theoretically analysed the results to explain the excellent laser performance. Analyses of losses caused by thermal effects and reabsorption are further needed to quantify the results better and find the optimum design. To ameliorate the low absorption rate of pump power, a residual pumping energy reuse system or pumping source with a narrower

Table 2
Parameters used in the simulation in Fig. 4(a). R_c is the reflectivity of the YLF crystal at ~600 nm.

T_{oc} (%)	γ	η_p	P_{tho} (W)	f_1	f_0	R_c (%)
8.9	0.040	0.732	0.433	0.591	2.796	3.7

linewidth could be applied.

CRediT authorship contribution statement

Xiuji Lin: Conceptualization, Methodology, Software, Formal analysis, Investigation, Data curation, Writing - original draft, Visualization. **Yao Zhu:** Investigation. **Shuaihao Ji:** Investigation. **Wensong Li:** Validation, Writing - review & editing. **Huiying Xu:** Resources, Supervision, Funding acquisition. **Zhiping Cai:** Resources, Supervision, Project administration, Funding acquisition.

Declaration of Competing Interest

The authors declare that they have no known competing financial interests or personal relationships that could have appeared to influence the work reported in this paper.

Acknowledgement

This work was supported by the National Natural Science Foundation of China (NSFC) (Grant Nos. 11674269, 61975168).

References

[1] R.G. Wheeland, Clinical uses of lasers in dermatology, Lasers Surg. Med. 16 (1) (1995) 2–23.
[2] F.A. L'Esperance, Clinical photocoagulation with the organic dye laser: a preliminary communication, Arch. Ophthalmol. 103 (9) (1985) 1312–1316.
[3] O. Halabi, N. Chiba, Efficient vector-oriented graphic drawing method for laser-scanned display, Displays 30 (3) (2009) 97–106.
[4] J.A. Creighton, DG Eadon. "Ultraviolet-visible absorption spectra of the colloidal metallic elements." J. Chem. Soc., Faraday Trans. 87 (1991).
[5] Y.C. Chi, D.H. Hsieh, C.Y. Lin, et al., Phosphorous diffuser diverged blue laser diode for indoor lighting and communication, Sci. Rep. 5 (2015) 18690.
[6] N. Niu, S. Pu, Q. Chen, et al., 302 nm continuous wave generation by intracavity frequency doubling of a diode-pumped Pr:YLF laser, Appl. Opt. 57 (33) (2018) 9798–9802.
[7] Y.F. Lü, X.H. Zhang, X.H. Fu, et al., Diode-pumped Nd: LuVO4 and Nd: YAG crystals yellow laser at 594 nm based on intracavity sum-frequency generation, Laser Phys. Lett. 7 (9) (2010) 634.
[8] Y.K. Bu, C.Q. Tan, N. Chen, Continuous-wave yellow light source at 579 nm based on intracavity frequency-doubled Nd: YLF/SrWO4/LBO Raman laser, Laser Phys. Lett. 8 (6) (2011) 439.
[9] X. Li, A.J. Lee, H.M. Pask, J.A. Piper, Y. HuoLi, Efficient, miniature, cw yellow source based on an intracavity frequency-doubled Nd:YVO4 self-Raman laser, Opt. Lett. 36 (8) (2011) 1428–1430.
[10] M.L. Rico, E. Moya, J.L. Valdes, et al., Continuous-wave yellow laser based on Nd-doped periodically poled lithium niobate, IEEE J. Sel. Top. Quantum Electron. 13 (3) (2007) 750–755.
[11] Y.F. Chen, Y.Y. Pan, Y.C. Liu, et al., Efficient high-power continuous-wave lasers at green-lime-yellow wavelengths by using a Nd:YVO4 self-Raman crystal, Opt. Express 27 (3) (2019) 2029–2035.
[12] T. Mao, Y. Duan, S. Chen, et al., Yellow and orange light selectable output generated by Nd: YAP/YVO4/LBO Raman laser, IEEE Photon. Technol. Lett. (2019).
[13] C. Kannengiesser, V. Ostroumov, V. Pfeufer, et al., Ten years optically pumped semiconductor lasers: review, state-of-the-art, and future developments." Solid State Lasers XIX: Technology and Devices, Int. Soc. Opt. Photon. 7578 (2010).
[14] W. Li, T. Du, J. Lan, et al., 716 nm deep-red passively Q-switched Pr:ZBLAN all-fiber laser using a carbon-nanotube saturable absorber, Opt. Lett. 42 (4) (2017) 671–674.
[15] D. Wu, Z. Cai, Y. Zhong, et al., 635-nm visible Pr3+-doped ZBLAN fiber lasers Q-switched by topological insulators SAs, IEEE Photon. Technol. Lett. 27 (22) (2015) 2379–2382.
[16] P.W. Metz, F. Reichert, F. Moglia, et al., High-power red, orange, and green Pr3+:LiYF4 lasers, Opt. Lett. 39 (2014) 3193–3196.
[17] T. Gün, P. Metz, G. Huber, Power scaling of laser diode pumped Pr3+:LiYF4 cw lasers: efficient laser operation at 522.6 nm, 545.9 nm, 607.2 nm, and 639.5 nm, Opt. Lett. 36 (6) (2011) 1002–1004.
[18] S. Luo, X. Yan, Q. Cui, et al., Power scaling of blue-diode-pumped Pr:YLF lasers at 523.0, 604.1, 606.9, 639.4, 697.8 and 720.9 nm, Opt. Commun. 380 (2016) 357–360.
[19] M. Fibrich, H. Jelínková, J. Šulc, et al., Visible cw laser emission of GaN-diode pumped Pr:YAlO 3 crystal, Appl. Phys. B 97 (2) (2009) 363.
[20] M. Fibrich, J. Šulc, H. Jelínková, "1-W level diode pumped Pr:YLF orange laser." Solid State Lasers XXV: Technology and Devices", Int. Soc. Opt. Photon. (2016) 9726.
[21] X.J. Lin, X.X. Huang, B. Liu, et al., Continuous-wave laser operation at 743 and 753 nm based on a diode-pumped c-cut Pr:YAlO3 crystal, Opt. Mater. 76 (2018) 16–20.
[22] H. Tanaka, S. Fujita, F. Kannari, High-power visibly emitting Pr3+:YLF laser end pumped by single-emitter or fiber-coupled GaN blue laser diodes, Appl. Opt. 57 (21) (2018) 5923–5928.
[23] B. Xu, Z. Liu, H.Y. Xu, et al., Highly efficient InGaN-LD-pumped bulk Pr:YLF orange laser at 607 nm, Opt. Commun. 305 (2013) 96–99.
[24] A.A. Kaminskii, H.J. Eichler, B. Liu, et al., LiYF4:Pr3+ laser at 639.5 nm with 30 J flashlamp pumping and 87 mJ output energy, Phys. Stat. Solidi (a) 138 (1) (1993) K45–K48.
[25] P. Laporta, M. Brussard, Design criteria for mode size optimization in diode-pumped solid-state lasers, IEEE J. Quantum Electron. 27 (10) (1991) 2319–2326.
[26] G. Shayeganrad, Efficient design considerations for end-pumped solid-state-lasers, Opt. Laser Technol. 44 (4) (2012) 987–994.
[27] D. Findlay, R.A. Clay, The measurement of internal losses in 4-level lasers, Phys. Lett. 20 (1966) 277–278.